Flux Expansion Nodal Method for Solving Static and Transient Neutron Diffusion Equations in Hexagonal-z Geometry

Xia Bangyang[1], Xie Zhongsheng[*1] , Xian Chunyu[2], Yao Dong[2]

[1]*Department of Nuclear Engineering, Xi'an Jiaotong University, Xi'an, Shaanxi 710049, China*

[2]*National Key Laboratory of Reactor System Design Technology, Chengdu, Sichuan 610041, China*

Abstract

An intranodal flux expansion nodal method (FENM) for solving static and transient neutron diffusion equations in hexagonal-z geometry has been developed, in which the flux distributions are expanded into a set of analytic basis functions and orthogonal second-order polynomials. In order to improve the nodal coupling relations, a new type of nodal boundary conditions is proposed, which requires the continuity of both the zero- and first-order moments of partial currents across the nodal surfaces. The numerical results for a series of benchmark problems demonstrate that FENM exhibits good accuracy and convergence.

KEYWORDS: Nodal Method, Neutron Diffusion Equation, Hexagonal Geometry, Analytic Basis Functions, First-Order Moments

1. Introduction

Recently, many modern advanced nodal methods have been developed and successfully applied to the analysis of the reactor cores with hexagonal assemblies. Among them the AFEN [1-3] and the ANC-H [4-5] are most noticeable, because they can eliminate the difficulties of performing transverse integration in hexagonal geometry and obtain the accurate solutions for various types of reactors.

In AFEN, the additional equations for the six corner-point fluxes of hexagonal node must be solved, which greatly increases the complexity of the solution. In this paper, similar to the AFEN method, FENM also solves diffusion equation directly, but in the FENM, a new type of nodal boundary conditions is proposed, which requires the continuity of both the zero- and first-order partial current moments across the interface simultaneously instead of the surface-averaged fluxes and corner-point fluxes, and this enables the full representation of the symmetries of hexagonal node. In comparison with AFEN, FENM has the following major features. (1) The new type of nodal boundary conditions is easily obtained and eliminates the difficulty and computational complexity of the solution to corner-point fluxes, and also considerably improves the nodal coupling relations. (2) The usage of the surface-averaged partial current moments considerably facilitates the utilization of the response matrix technique for the iterative solution and improves the computational efficiency. These features of FENM make it possible to provide good accuracy and efficiency for solving neutron diffusion equations in hexagonal-z geometry.

In the second part of this paper, based on FENM an efficient nodal method for numerical

Corresponding author, Tel. +86-29-8266-9245; Fax. +86-29-8266-7802, E-mail address. zsxie@mail.xjtu.edu.cn

solution of space-time kinetics equation in hexagonal-z geometry is proposed. In this method, the static diffusion equation with fixed source term obtained after temporal discretization is solved by FENM. The fixed source term and the delayed neutron precursor concentration are approximated in terms of second-order polynomials. The response matrix technique is used for the iterative solution of space-time kinetics equation.

2. Method for solving static diffusion equation

2.1 Intranodal flux distributions

The matrix form of the static neutron diffusion equations in hexagonal-z geometry can be written as:

$$-\nabla^2 \mathbf{\Phi}(\mathbf{r}) + \sum(k_{eff})\mathbf{\Phi}(\mathbf{r}) = 0 \qquad (1)$$

where $\mathbf{\Phi}(\mathbf{r}) = col\{\Phi_1(\mathbf{r}), \Phi_2(\mathbf{r}), ..., \Phi_G(\mathbf{r})\}$ is the neutron flux and the matrix $\sum(k_{eff})$ is a square matrix of order G with its elements $\sum_{gg'}$ as follows:

$$\sum_{gg'} = (\delta_{gg'} \sum_{tg} - \sum^{s}_{gg'} - \frac{\chi_g}{k_{eff}} \nu \sum_{fg'}) / D_g \qquad (2)$$

where $\delta_{gg'}$ is the Kronecker symbol and the other notations are standard.

Figure 1: Coordinate system for the hexagonal node

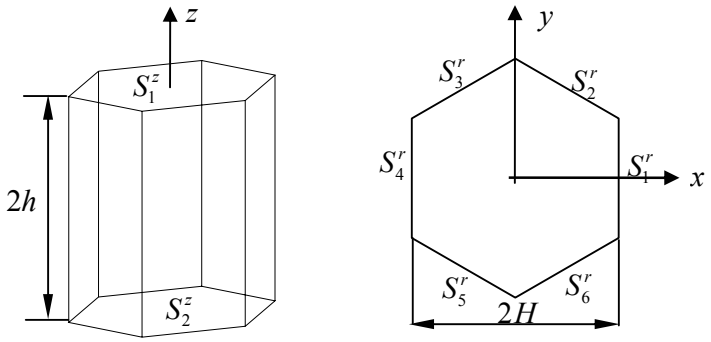

Figure 2: The positive and negative half-nodal surfaces

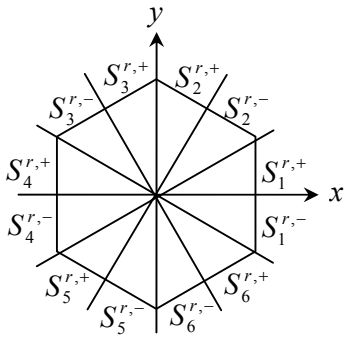

The analytic solution of Eq. (1) is dictated by the eigenvalues λ_m and the corresponding eigenvectors $\mathbf{u}_m$ of the matrix $\sum(k_{eff})$. Eq. (1) can be solved without any difficulties if all eigenvalues λ_m are real, however, for general multigroup problems some of the

eigenvalues λ_m may be complex. Therefore, in the following discussion different treatments are described for these two cases.

If all eigenvalues λ_m of matrix $\sum(k_{eff})$ are real, we can use the following transformation

$$\mathbf{U} = [\mathbf{u}_1, \mathbf{u}_2, ..., \mathbf{u}_G], \mathbf{\Psi}(\mathbf{r}) = \mathbf{U}^{-1}\mathbf{\Phi}(\mathbf{r}) \tag{3}$$

to reduce Eq. (1) to a decoupled form

$$-\nabla^2 \Psi_m(\mathbf{r}) + \lambda_m \Psi_m(\mathbf{r}) = 0, m = 1,...,G \tag{4}$$

where the matrix $\mathbf{U}$ is a $(G \times G)$ matrix. The analytic solution to Eq. (4) can be easily found and written as [2, 3]

$$\Psi_m(\mathbf{r}) = \sum_{l=1}^{\infty} [A_{ml}^{\infty} e^{\sqrt{\lambda_m}\mathbf{e}_l\mathbf{r}} + B_{ml}^{\infty} e^{-\sqrt{\lambda_m}\mathbf{e}_l\mathbf{r}}] \tag{5}$$

where $\mathbf{e}_l$ is an arbitrary unit vector. In practical calculations, the number of the terms in Eq. (5) mainly depends on the number of the available nodal boundary conditions. In general, increasing the number of the boundary conditions will obtain more accurate results, but the computing times also increase. In this paper, 8 interface partial currents and 10 first-order moments of the interface partial currents are adopted as the boundary conditions. The practical experience of previous works [2,3,6] shows that these numbers of boundary conditions can provide sufficient accuracy. Considering the coordinate system in Fig.1 and the symmetry property of hexagonal node, the following nine $\mathbf{e}_l$ unit vectors are used for Eq. (5)

$$\mathbf{e}_l = \cos[\frac{(2l-3)\pi}{12}] e_x + \sin[\frac{(2l-3)\pi}{12}] e_y, \quad l = 1,2,...,6 \tag{6-1}$$

$$\mathbf{e}_l = \mathbf{e}_z, \quad l = 7 \tag{6-2}$$

$$\mathbf{e}_l = \cos\frac{\pi}{4}\mathbf{e}_z + \sin\frac{\pi}{4}\mathbf{e}_x, \quad l = 8 \tag{6-3}$$

$$\mathbf{e}_l = \cos\frac{\pi}{4}\mathbf{e}_z + \sin\frac{\pi}{4}\mathbf{e}_y, \quad l = 9 \tag{6-4}$$

where $\mathbf{e}_x$, $\mathbf{e}_y$ and $\mathbf{e}_z$ are the unit vectors of coordinate axes x, y and z respectively. So that $\Psi_m(\mathbf{r})$ can be written in the following form:

$$\Psi_m(\mathbf{r}) = \sum_{l=1}^{9} A_{ml} SN(k_m \mathbf{e}_l \mathbf{r}) + \sum_{l=1}^{9} B_{ml} CS(k_m \mathbf{e}_l \mathbf{r}) \tag{7}$$

where $k_m = \sqrt{|\lambda_m|}$, and SN, CS denotes $\sinh$, $\cosh$ if $\lambda_m > 0$ and $\sin$, $\cos$ if $\lambda_m < 0$, respectively. By using Eq. (3) and Eq. (7), the intranodal flux distribution $\Phi_g(\mathbf{r})$ can be obtained:

$$\Phi_g(\mathbf{r}) = \sum_{m=1}^{G} u_{gm} \{\sum_{l=1}^{9} A_{ml} SN(k_m \mathbf{e}_l \mathbf{r}) + \sum_{l=1}^{9} B_{ml} CS(k_m \mathbf{e}_l \mathbf{r})\} \tag{8}$$

where u_{gm} is the element of the matrix $\mathbf{U}$ defined in Eq. (3).

If some of these eigenvalues λ_m are complex numbers, the complex basis functions will

appear, which can't be handled effectively. Here a new treatment, which is proposed by Cho[3], is adopted to treat this case. Because the matrix $\sum(keff)$ is real, the complex eigenvalues and the corresponding eigenvectors must appear in conjugate pairs. Suppose λ_1 and λ_2 are the two complex conjugate eigenvalues, the corresponding eigenvectors $\mathbf{u_1}$ and $\mathbf{u_2}$ are also conjugates. We introduce a new transformation $\mathbf{U}^*$

$$\mathbf{U}^* = \left[\mathrm{Re}(\mathbf{u}_1), \mathrm{Im}(\mathbf{u}_1), \mathbf{u}_3, \cdots, \mathbf{u}_\mathbf{G}\right] \tag{9}$$

$$\mathbf{\Psi}(\mathbf{r}) = \mathbf{U}^{*-1}\mathbf{\Phi}(\mathbf{r}) \tag{10}$$

where $\mathrm{Re}(\mathbf{u}_1)$ and $\mathrm{Im}(\mathbf{u}_1)$ denote the real and imaginary parts of the vector $\mathbf{u_1}$, respectively. After some algebraic manipulations, the intranodal flux distribution $\Phi_g(\mathbf{r})$ can be obtained for this case [3]:

$$\Phi_g(\mathbf{r}) = \sum_{m=1}^{2} u_{gm}^* \Psi_m(\mathbf{r}) + \sum_{m=3}^{G} u_{gm}^* \cdot\{\sum_{l=1}^{9} A_{ml} SN(k_m \mathbf{e}_l \mathbf{r}) + \sum_{l=1}^{9} B_{ml} CS(k_m \mathbf{e}_l \mathbf{r})\} \tag{11}$$

with

$$\begin{aligned}\Psi_1(\mathbf{r}) = &\sum_{l=1}^{9} A_{1l}\cosh(p\mathbf{e}_l\mathbf{r})\cos(q\mathbf{e}_l\mathbf{r}) + \sum_{l=1}^{9} B_{1l}\sinh(p\mathbf{e}_l\mathbf{r})\sin(q\mathbf{e}_l\mathbf{r}) \\ &+ \sum_{l=1}^{9} A_{2l}\sinh(p\mathbf{e}_l\mathbf{r})\cos(q\mathbf{e}_l\mathbf{r}) + \sum_{l=1}^{9} B_{2l}\cosh(p\mathbf{e}_l\mathbf{r})\sin(q\mathbf{e}_l\mathbf{r})\end{aligned} \tag{12}$$

$$\begin{aligned}\Psi_2(\mathbf{r}) = &-\sum_{l=1}^{9} A_{1l}\sinh(p\mathbf{e}_l\mathbf{r})\sin(q\mathbf{e}_l\mathbf{r}) + \sum_{l=1}^{9} B_{1l}\cosh(p\mathbf{e}_l\mathbf{r})\cos(q\mathbf{e}_l\mathbf{r}) \\ &- \sum_{l=1}^{9} A_{2l}\cosh(p\mathbf{e}_l\mathbf{r})\sin(q\mathbf{e}_l\mathbf{r}) + \sum_{l=1}^{9} B_{2l}\sinh(p\mathbf{e}_l\mathbf{r})\cos(q\mathbf{e}_l\mathbf{r})\end{aligned} \tag{13}$$

2.2 Nodal boundary conditions

In this paper, we consider18 boundary conditions that constrain the intranodal flux distributions in the hexagonal-z node shown in Fig. 1, which include 8 surface-averaged partial currents, 6 radial first-order partial current moments and 4 axial first-order partial current moments.

In the radial direction, the zero- and first-order moments of partial currents at given surface S_k^r are defined as:

$$\bar{J}_{g,k}^{r0,\pm} = \frac{1}{4}\bar{\Phi}_{g,k}^{r0} \pm \frac{1}{2}\bar{J}_{g,k}^{r0}, \quad k = 1,2,...,6 \tag{14}$$

$$\bar{J}_{g,k}^{r1,\pm} = \frac{1}{S_k^r}\int_{S_k^r} \mathrm{sgn}(\mathbf{r}) J_{g,k}^{r0,\pm}(\mathbf{r}) d\mathbf{r}\,, \mathbf{r} \in S_k^r \text{ and } k = 1,2,...,6 \tag{15}$$

with the sign function $\mathrm{sgn}(\mathbf{r})$ as:

$$\mathrm{sgn}(\mathbf{r}) = \begin{cases} +1 & \mathbf{r} \in S_k^{r,+} \\ -1 & \mathbf{r} \in S_k^{r,-} \end{cases} \tag{16}$$

where $S_k^{r,+}$ and $S_k^{r,-}$ are the positive and negative half-nodal surfaces shown in Fig 2. The

$\overline{\Phi}_{g,k}^{r0}$ and $\overline{J}_{g,k}^{r0}$ represent the neutron flux and current averaged over the surface S_k^r respectively.

In the axial direction, the zero- and first-order moments of partial currents at the given surface S_k^z is defined as:

$$\overline{J}_{g,k}^{z0,\pm} = \frac{1}{4}\overline{\Phi}_{g,k}^{z0} \pm \frac{1}{2}\overline{J}_{g,k}^{z0} \tag{17}$$

$$\overline{J}_{g,k}^{zx1,\pm} = \frac{1}{S_k^z}\int_{-H}^{+H}\int_{-y_s(x)}^{+y_s(x)} \mathrm{sgn}(x) J_{g,k}^{z0,\pm}(x,y,z)dydx\,|_{z=z_k} \tag{18}$$

$$\overline{J}_{g,k}^{zy1,\pm} = \frac{1}{S_k^z}\int_{-H}^{+H}\int_{-y_s(x)}^{+y_s(x)} \mathrm{sgn}(y) J_{g,k}^{z0,\pm}(x,y,z_k)dydx\,|_{z=z_k} \tag{19}$$

where the function $y_s(x) = (H - |x|)/\sqrt{3}$.

Obviously, all the zero and first moments of currents are the functions of the flux expansion coefficients $\mathrm{A_{ml}}$ and $\mathrm{B_{ml}}$.

2.3 Iteration solution procedure

Based on the intranodal flux expansion (8), (11) and the definitions of the partial currents moments (14), (15), (17), (18) and (19), we can obtain the following two matrix equations that relate both the partial current moments and the intranodal flux expansion coefficients:

$$\overline{\mathbf{J}}^{-} = \mathbf{Q}^{-}\mathbf{C} \tag{20}$$

$$\overline{\mathbf{J}}^{+} = \mathbf{Q}^{+}\mathbf{C} \tag{21}$$

where the partial current moments vector $\overline{\mathbf{J}}^{\pm} = [(\overline{J}_{1,1}^{r0,\pm},...,\overline{J}_{1,6}^{r0,\pm},\overline{J}_{1,1}^{r1,\pm},...,\overline{J}_{1,6}^{r1,\pm},\overline{J}_{1,1}^{z0,\pm},\overline{J}_{1,2}^{z0,\pm},\overline{J}_{1,1}^{zx1,\pm},\overline{J}_{1,2}^{zx1,\pm},\overline{J}_{1,1}^{zy1,\pm},\overline{J}_{1,2}^{zy1,\pm}),...,(\overline{J}_{G,1}^{r0,\pm},...,\overline{J}_{G,6}^{r0,\pm},\overline{J}_{G,1}^{r1,\pm},...,\overline{J}_{G,6}^{r1,\pm},\overline{J}_{G,1}^{z0,\pm},\overline{J}_{G,2}^{z0,\pm},\overline{J}_{G,1}^{zx1,\pm},\overline{J}_{G,2}^{zx1,\pm},\overline{J}_{G,1}^{zy1,\pm},\overline{J}_{G,2}^{zy1,\pm})]^T$ and the flux expansion coefficients $\mathbf{C} = [(A_{11},...,A_{19},B_{11},...,B_{19}),...,(A_{G1},...,A_{G9},B_{G1},...,B_{G9})]^T$. Both the matrices $\mathbf{Q}^{+}$ and $\mathbf{Q}^{-}$ are the constant matrices whose element depend on k_{eff} and the group constants of the node.

To determine the flux expansion coefficients $\mathbf{C}$, the inverse matrix $\mathbf{Q}^{-1}$ of the matrix $\mathbf{Q}^{-}$ needs to be calculated. Once the matrix $\mathbf{Q}^{-1}$ is obtained, the intranodal flux expansion coefficients can be expressed in terms of the incoming partial current moments:

$$\mathbf{C} = \mathbf{Q}^{-1}\overline{\mathbf{J}}^{-} \tag{22}$$

Then inserting Eq. (22) into Eq. (21) yields the response matrix equation as follows:

$$\overline{\mathbf{J}}^{+} = \mathbf{Q}^{+}\mathbf{Q}^{-1}\overline{\mathbf{J}}^{-} \tag{23}$$

According to the continuity conditions of $\overline{\mathbf{J}}^{+}$ and $\overline{\mathbf{J}}^{-}$ at each surface, Eq. (23) forms a closed and complete system of equations. Concerning the core boundary conditions, in general, the albedos α are given for each group at the core external surfaces, so the following expression can be obtained:

$$\overline{J}_{g,k}^{s,-} = R\overline{J}_{g,k}^{s,+} \tag{24}$$

where $R=(1+2\alpha)/(1-2\alpha)$ and the superscript (s) refers to the radial and axial partial currents moments defined above at surfaces. Eqs. (22) ~(23) together with aforementioned interface conditions represent the equations for the iteration solution. Given an initial value of multiplication factor, the matrix eigenvalues problem of the matrix $\sum(k_{eff})$ is firstly solved for eigenvalues λ_m and eigenvectors $\mathbf{u}_m$, and the response matrices $\mathbf{Q}^{+}\mathbf{Q}^{-I}$ are calculated. Then the outgoing partial current moments are obtained by all nodal sweeps from the initially given or previously updated incoming currents moments by using Eq. (23) and Eq. (24), at the end of sweeps the effective multiplication factor is calculated. The iteration procedure is accelerated by Chebychev extrapolation and the coarse-mesh rebalancing method.

3. Method for solving transient equation

3.1 Discretization of kinetics equation

The reactor kinetics diffusion equation may be written as follows:

$$\frac{1}{v_g}\frac{\partial\Phi_g(\mathbf{r},t)}{\partial t}=\nabla D_g(t)\nabla\Phi_g(\mathbf{r},t)-\sum_{tg}(t)\Phi_g(\mathbf{r},t)+\sum_{g'=1}^{G}\sum_{gg'}(t)\Phi_{g'}(\mathbf{r},t)$$
$$+\chi_{dg}\sum_{i=1}^{I}\lambda_i C_i(\mathbf{r},t)+(1-\beta)\chi_{pg}\sum_{g'=1}^{G}\nu\sum_{fg'}(t)\Phi_{g'}(\mathbf{r},t) \qquad (25\text{-}1)$$

$$\frac{\partial C_i(\mathbf{r},t)}{\partial t}=\beta_i\sum_{g'=1}^{G}\nu\sum_{fg'}(t)\Phi_{g'}(\mathbf{r},t)-\lambda_i C_i(\mathbf{r},t),\ i=1,2,...,I \qquad (25\text{-}2)$$

where $\Phi_g(\mathbf{r},t)$ and $C_i(\mathbf{r},t)$ are the group g flux and the type i delayed neutron precursor density, and the other notations are standard.

A fully implicit temporal integration of Eq (25) over the time interval between (t_{n-1},t_n) leads to

$$\frac{1}{v_g\Delta t_n}\Phi_g(\mathbf{r},t_n)-\nabla\cdot D_g(\mathbf{r},t_n)\nabla\Phi_g(\mathbf{r},t_n)+\Sigma_{tg}(\mathbf{r},t_n)\Phi_g(\mathbf{r},t_n)$$
$$=\sum_{g'=1}^{G}\Sigma_{g'g}(\mathbf{r},t_n)\Phi_{g'}(\mathbf{r},t_n)+\overline{\chi}_g\sum_{g'=1}^{G}\nu\Sigma_{fg'}(\mathbf{r},t_n)\Phi_{g'}(\mathbf{r},t_n)+S_g^{eff}(\mathbf{r},t_n) \qquad (26\text{-}1)$$

$$C_i(r,t_n)=C_i(r,t_{n-1})e^{-\lambda_i\Delta t_n}+F_{i_n}^{0}\sum_{g'=1}^{G}\nu\Sigma_{fg'}(r,t_{n-1})\Phi_{g'}(r,t_{n-1})$$
$$+F_{i_n}^{1}\sum_{g'=1}^{G}\nu\Sigma_{fg'}(r,t_n)\Phi_{g'}(r,t_n) \qquad (26\text{-}2)$$

where $F_{i_n}^{0}$ and $F_{i_n}^{1}$ are constants.

$$S_g^{eff}(\mathbf{r},t_n)=\frac{1}{v_g\Delta t_n}\Phi_g(\mathbf{r},t_{n-1})+\sum_{i=1}^{I}\chi_{dgi}\lambda_i C_i(\mathbf{r},t_{n-1})e^{-\lambda_i\Delta t_n}$$
$$+\sum_{i=1}^{I}\chi_{dgi}\lambda_i F_{i_n}^{0}\cdot\sum_{g'=1}^{G}\nu\Sigma_{fg'}(\mathbf{r},t_{n-1})\Phi_{g'}(\mathbf{r},t_{n-1}) \qquad (26\text{-}3)$$

Then put Eq. (26-1) into the matrix form:

$$-\mathbf{D}(t_n)\nabla^2\mathbf{\Phi}(\mathbf{r},t_n)+\mathbf{\Lambda}(t_n)\mathbf{\Phi}(\mathbf{r},t_n)=\mathbf{S}^{eff}(\mathbf{r},t_n) \qquad (27)$$

The general solution of Eq. (27) can be found as a sum of the homogeneous solution $\mathbf{\Phi}_a(\mathbf{r},t_n)$ to the Helmholtz equation:

$$-\mathbf{D}(t_n)\nabla^2\mathbf{\Phi}_a(\mathbf{r},t_n)+\mathbf{\Lambda}(t_n)\mathbf{\Phi}_a(\mathbf{r},t_n)=0 \tag{28}$$

and the particular solution $\mathbf{\Phi}_p(\mathbf{r},t_n)$ to the following equation:

$$-\mathbf{D}(t_n)\nabla^2\mathbf{\Phi}_p(\mathbf{r},t_n)+\mathbf{\Lambda}(t_n)\mathbf{\Phi}_p(\mathbf{r},t_n)=\mathbf{S}^{eff}(\mathbf{r},t_n) \tag{29}$$

We note that Eq. (28) is the same as the static diffusion equation (1), so the analytic solution of Eq. (28) can be obtained by use of the method FENM mentioned above. The particular solution $\mathbf{\Phi}_p(\mathbf{r},t_n)$ and the fixed source term $\mathbf{S}^{eff}(\mathbf{r},t_n)$ are approximated by a polynomial expansion up to the second order:

$$\mathbf{\Phi}_p(\mathbf{r},t_n)=\sum_{l=1}^{8}\mathbf{c}_{pl}^{n}w_l(\mathbf{r}) \tag{30}$$

$$\mathbf{S}^{eff}(\mathbf{r},t_n)=\sum_{l=1}^{8}\mathbf{s}_{l}^{n}w_l(\mathbf{r}) \tag{31}$$

with the polynomial $w_l(\mathbf{r})$ [6]

$$w_1(\mathbf{r})=1/N_1, w_2(\mathbf{r})=x/N_2, w_3(\mathbf{r})=y/N_3, w_4(\mathbf{r})=(x^2+y^2-5H^2/9)/N_4,$$

$$w_5(\mathbf{r})=(x^2-y^2)/N_5, w_6(\mathbf{r})=2xy/N_5\ w_7(\mathbf{r})=z/N_7, w_8(\mathbf{r})=(3z^2-h^2)/N_8. \tag{32}$$

where the nominalization factors N_l are obtained by the following orthogonality relation:

$$\int_V w_i.w_j dV=\delta_{ij} \tag{33}$$

3.2 Determining the coefficients of the flux expansions and iteration solution procedure

Firstly, the coefficients $\mathbf{s}_l^n$ of the fixed source term $\mathbf{S}^{eff}(\mathbf{r},t_n)$ are determined by use of the following weighted integral:

$$s_{gl}^{n}=\int_V w_l(\mathbf{r}).\sum_{l=1}^{8}\mathbf{s}_l^n w_l(\mathbf{r})d\mathbf{r}=\int_V w_l(\mathbf{r}).S_g^{eff}(\mathbf{r},t_n)d\mathbf{r}\ \square\ \mathbf{r}\in V \tag{34}$$

then substituting Eqs. (30), (31) into the Eq. (29) leads to

$$-\frac{4\mathbf{D}(\mathrm{t_n})}{\mathrm{N_4}}\mathbf{c}_{\mathrm{p4}}^{\mathrm{n}}+\frac{6\mathbf{D}(\mathrm{t_n})}{\mathrm{N_8}}\mathbf{c}_{\mathrm{p8}}^{\mathrm{n}}+\Lambda(\mathrm{t_n})\sum_{\mathrm{l=1}}^{8}\mathbf{c}_{\mathrm{pl}}^{\mathrm{n}}\mathrm{w_1}(\mathbf{r})=\sum_{\mathrm{l=1}}^{8}\mathbf{s}_{\mathrm{l}}^{\mathrm{n}}\mathrm{w_1}(\mathbf{r}) \tag{35}$$

If two sides of Eq. (35) multiply the polynomial $w_l(\mathbf{r})$ and integrate on the node volume at the same time, the coefficients $\mathbf{c}_{pl}^n$ of the particular solution $\mathbf{\Phi}_p(\mathbf{r},t_n)$ can be obtained.

Using the nodal boundary conditions, the following two matrix equations similar to Eq. (20) and Eq. (21) can be obtained:

$$\mathbf{J}^{+}(t_n)=\mathbf{Q}_a^{n,+}\mathbf{C}_a^n+\mathbf{Q}_p^{n,+}\mathbf{C}_p^n \tag{36}$$

$$\mathbf{J}^{-}(t_n)=\mathbf{Q}_a^{n,-}\mathbf{C}_a^n+\mathbf{Q}_p^{n,-}\mathbf{C}_p^n \tag{37}$$

where the matrices $\mathbf{Q}_a^{n,+}, \mathbf{Q}_a^{n,-}, \mathbf{Q}_p^{n,+}$ and $\mathbf{Q}_p^{n,-}$ are the constant matrices whose element depend on the group constants of the node, the time step size and the kinetics parameters. The vectors $\mathbf{C}_a^n$ and $\mathbf{C}_p^n$ are composed of the coefficients of the homogeneous solution $\mathbf{\Phi}_a(\mathbf{r},t_n)$ and the particular solution $\mathbf{\Phi}_p(\mathbf{r},t_n)$ respectively.

The coefficients $\mathbf{C}_a^n$ of the homogeneous solution $\mathbf{\Phi}_a(\mathbf{r},t_n)$ are determined in the same manner as used in the static calculation. Using Eq. (37), $\mathbf{C}_a^n$ can be expressed by the incoming partial current moments $\mathbf{J}^-(t_n)$ as:

$$\mathbf{C}_a^n = \mathbf{Q}_a^{n,-I}[\mathbf{J}^-(t_n) - \mathbf{Q}_p^{n,-}\mathbf{C}_p^n] \tag{38}$$

Once $\mathbf{J}^-(t_n)$ is determined, the coefficients $\mathbf{C}_a^n$ can be calculated easily. Then inserting Eq. (38) into Eq. (36) yields the response matrix equation similar to Eq. (23):

$$\mathbf{J}^+(t_n) = \mathbf{Q}_a^{n,+}\mathbf{Q}_a^{n,-I}\mathbf{J}^-(t_n) + [\mathbf{Q}_p^{n,+} - \mathbf{Q}_p^{n,-}\mathbf{Q}_a^{n,+}\mathbf{Q}_a^{n,-I}]\mathbf{C}_p^n \tag{39}$$

Eqs. (34), (35), (38) and (39) together with the nodal boundary conditions represent the equations for the iteration solution.

4. Numerical results

Firstly, the FENM has been tested against a series of two- and three-dimensional steady -state benchmark problems [5]. These numerical results presented in Table.1 and Table.2 demonstrate that FENM exhibits excellent accuracy. The maximum and average node power prediction errors of FENM are less than 1% and 0.4% for two- dimensional benchmark problems, and less than 2.5% and 0.6% for three-dimensional benchmark problems, respectively. The numerical results of AFEN and ANC-H are taken from Ref [7].

Figure 3: Sixty-degree core sector for the transient test problem

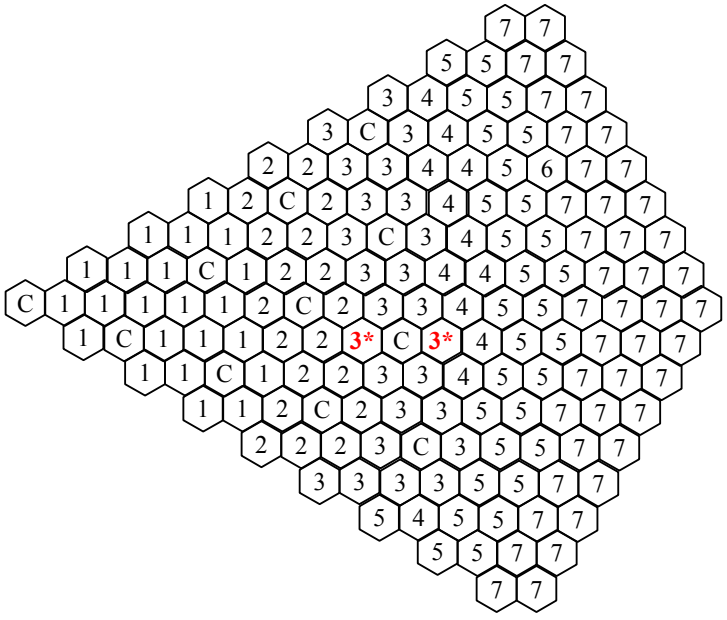

Figure 4: Core Power vs. time for the transient test problem

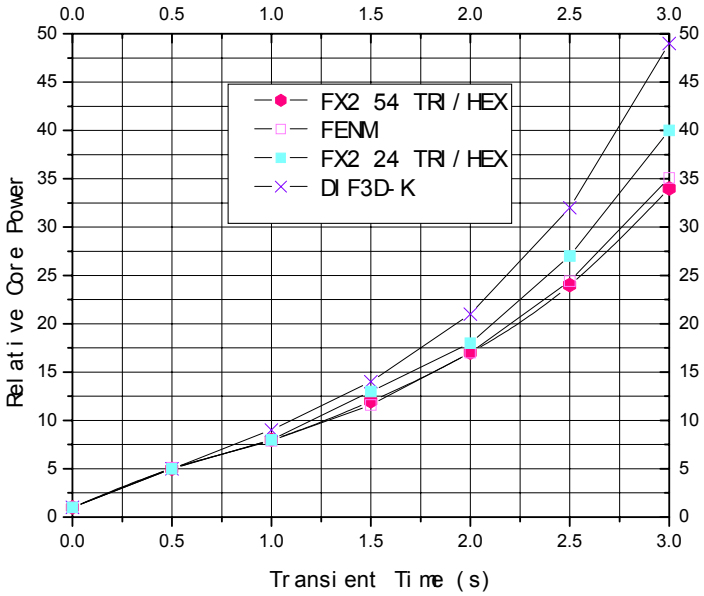

Table 1: Numerical results of the steady-state 2D hexagonal benchmark problems

Benchmark Problems	Method	Δk_{eff} (pcm)	$\varepsilon_{\max}$ (%)	ε_{avg} (%)
VVER-440 (α□0.5)	FENM	-5.0	0.51	0.15
	AFEN	23.0	1.25	0.52
	ANC-H	29.0	0.82	-
VVER-1000 (α□0.5)	FENM	5.0	0.87	0.28
	AFEN	32.0	3.73	1.52
	ANC-H	7.0	0.7	-
VVER-1000 (α□0.125)	FENM	3.0	-0.43	0.17
	AFEN	22.0	1.20	0.60
	ANC-H	16.0	0.7	-
IAEA without reflector (α□0.5)	FENM	13.0	0.43	0.17
	AFEN	49.0	2.31	1.10
	ANC-H	-7.0	0.8	-
IAEA without reflector (α□0.125)	FENM	11.0	-0.21	0.08
	AFEN	17.0	0.86	0.33
	ANC-H	6.0	0.5	-
IAEA with reflector (α□0.5)	FENM	-11.0	0.67	0.30
	AFEN	58.7	2.01	0.96
	ANC-H	-2.0	0.7	-
IAEA with reflector (α□0.125)	FENM	9.0	0.73	0.32
	AFEN	43.7	1.55	0.72
	ANC-H	7.0	0.5	-

Table 2: Numerical results of the steady-state 3D hexagonal benchmark problems

Benchmark Problems	Method	Δk_{eff} (pcm)	$\varepsilon_{\max}$ (%)	ε_{avg} (%)
VVER-440	FENM	26.0	2.35	0.58
	AFEN	30.0	3.20	0.73
	ANC-H	25.0	1.28	-
VVER-1000	FENM	15.0	1.40	0.47
	AFEN	11.0	1.70	0.81
	ANC-H	13.0	0.90	-

The transient test problem is a two-dimensional problem taken from Ref [8], which models the dropping of two fuel bearing rods (indicated by 3*, per 60-degree sector) into outer control gang as shown in Fig.3, producing a local perturbation in the flux peaked region. The duration of the drop is 0.205s. Cross section data and kinetics parameters are also taken from Ref [8]. Fig.4 shows the core power variation estimated by FENM and comparison with results of DIF3D-K and fine mesh code FX2-TH. From these results, it is evident that the FENM solution is clossed to FX2 54Tri/Hex and more accurate than the 24 Tri/Hex FX2-TH solution.

5. Conclusions

A new hexagonal nodal method for solving static and transient neutron diffusion equations, which is based on expanding the intranodal flux distributions into analytic basis functions (FENM), is presented in this paper. In this method the nodes are coupled through the zero- and first-order partial current moments at nodal interfaces simultaneously, and the response matrix technique, which is a very efficient scheme for the diffusion calculation ,is used for the iterative solution of diffusion equation. The numerical results for a series of static and transient benchmark problems demonstrate that it is a very accurate and efficient method for the prediction of criticality and power distribution in the reactors with hexagonal assemblies.

Reference

1) N. Z. Cho, J. M. Noh. The AFEN method for hexagonal nodal calculation and reconstruction. Trans.Am.Nucl.Soc., **71**,466(1994).
2) N. Z. Cho, J. M. Noh. Analytic function expansion nodal method for hexagonal geometry. Nucl.Sci.Eng., **121**, 245(1995).
3) N. Z. Cho, Y. H. Kim, K.W. Park. Extension of analytic function expansion nodal method to multigroup problems in hexagonal-z geometry. Nucl.Sci.Eng., **126**, 35(1995).
4) Y. A. Chao, N. Tsolfanidis. Conformal mapping and hexagonal nodal methods –I: mathematical foundation. Nucl.Sci.Eng., **121**, 202(1995).
5) Y.A. Chao, Y. A. Shatilla. Conformal mapping and hexagonal nodal methods - II: implemen -tation in the ANC-H code. Nucl.Sci.Eng., **121**, 210(1995).
6) U. Grundmann, F. Hollstein. A two-dimensional intranodal flux expansion method for hexagonal geometry. Nucl.Sci.Eng., **133**, 201(1999).
7) J. Y. Cho, C. H. Kim. Higher order Polynomial expansion nodal method for hexagonal

core neutronics analysis. Ann.Nucl.Energy, **25**, 1021(1998).

8) T. A. Taiwo, H. S. Khalil. The DIF3D-K: A nodal kinetics code for solving the time-dependent diffusion equation. Proc. of Int. Conf. on Mathematics and Computations, Reactor Physics, and Environmental Analysis, Portland, Oregon, **2**,1171(1995).
9) B. Xia, Z. Xie, Flux expansion nodal method for solving multigroup neutron diffusion equations in hexagonal-z geometry. Ann.Nucl.Energy, **33**, 370(2006).